Nanoscale

PAPER

Cite this: *Nanoscale*, 2015, **7**, 13694

Solution-processed assembly of ultrathin transparent conductive cellulose nanopaper embedding AgNWs†

Yuanyuan Song,[a] Yaoquan Jiang,[b] Liyi Shi,[b] Shaomei Cao,[b] Xin Feng,*[a,b] Miao Miao[b] and Jianhui Fang[c]

Received 16th May 2015,
Accepted 3rd July 2015

DOI: 10.1039/c5nr03218k

www.rsc.org/nanoscale

Natural biomass based cellulose nanopaper is becoming a promising transparent substrate to supersede traditional petroleum based polymer films in realizing future flexible paper-electronics. Here, ultrathin, highly transparent, outstanding conductive hybrid nanopaper with excellent mechanical flexibility was synthesized by the assembly of nanofibrillated cellulose (NFC) and silver nanowires (AgNWs) using a pressured extrusion paper-making technique. The hybrid nanopaper with a thickness of 4.5 μm has a good combination of transparent conductive performance and mechanical stability using bamboo/hemp NFC and AgNWs cross-linked by hydroxypropylmethyl cellulose (HPMC). The heterogeneous fibrous structure of BNFC/HNFC/AgNWs endows a uniform distribution and an enhanced forward light scattering, resulting in high electrical conductivity and optical transmittance. The hybrid nanopaper with an optimal weight ratio of BNFC/HNFC to AgNWs shows outstanding synergistic properties with a transmittance of 86.41% at 550 nm and a sheet resistance of 1.90 ohm sq^{-1}, equal to the electronic conductivity, which is about 500 S cm^{-1}. The BNFC/HNFC/AgNW hybrid nanopaper maintains a stable electrical conductivity after the peeling test and bending at 135° for 1000 cycles, indicating remarkably strong adhesion and mechanical flexibility. Of importance here is that the high-performance and low-cost hybrid nanopaper shows promising potential for electronics application in solar cells, flexible displays and other high-technology products.

Introduction

Transparent conductive films fabricated on plastic substrates have received considerable attention in recent years because of their simple processing and low manufacturing costs.[1] However, the great challenge for transparent conductive plastic films is to sustain excellent mechanical durability and electrical continuity upon repeated bending or high temperature processing.[2] The device performance is strongly related to the improved tolerance for heat distortion and dimensional stability of plastic films during large temperature changes. Therefore, it is desirable to find a strong competitive replacement with excellent thermal stability that can be bent and even fully folded. Owing to its lightweight, flexibility, low thermal expansion, biodegradability, renewability, and enhanced printability, optical transparent nanopaper based on nanofibrillated cellulose (NFC) is emerging as an ideal platform with the potential to supersede petroleum-based polymers in the future production of next-generation flexible and wearable electronics.[3–5] NFC nanopaper from abundant natural biomass is a suitable building block to house a range of guest functional materials for flexible matrices with exciting synergistic properties.[6] Generally, indium tin oxide (ITO) has been widely used as a transparent conductor due to its high transparency and low sheet resistance (over 80% and below 30 ohm sq^{-1}) on a flexible substrate,[7,8] but the inherent brittleness of ITO usually causes cracks upon bending or folding.[9,10] To solve these problems, great effort has been made to explore practical alternatives such as conducting polymers,[11,12] graphene,[13–15] carbon nanotubes,[16–18] and metal nanowires[19,20] for flexible transparent conductive films. Silver nanowires (AgNWs) are among the most promising candidates because of their exceptional transparency and high conductivity (95% and 20 ohm sq^{-1}).[21–23] Considerable attention has been devoted to directly depositing conductive materials on the surface of flexible substrates using Mayer rod coating,[24,25] wet coating,[26–28] and vacuum filtration.[29–31] The significant challenge in meeting

[a]*School of Materials Sciences and Engineering, Shanghai University, Shanghai 200444, P. R. China. E-mail: fengxin@shu.edu.cn; Fax: +86-21-66136038; Tel: +86-21-66137257*
[b]*Research Center of Nano Science and Technology, Shanghai University, Shanghai 200444, P. R. China*
[c]*Department of Chemistry, Shanghai University, Shanghai 200444, P. R. China*
†Electronic supplementary information (ESI) available. See DOI: 10.1039/c5nr03218k

This journal is © The Royal Society of Chemistry 2015

the requirements of strong adhesion between conductive materials and transparent substrates needs to be addressed.[32] In addition, pure AgNW films can be easily oxidized to corrosion due to long time exposure in ambient air.[33,34] Therefore, the development of hybrid transparent conductive films with high performance by encapsulating AgNWs is becoming an important research issue.[35] Chun *et al.* prepared a hybrid Ag-MWNT composite film with an average thickness of 140 μm by drop casting using a polyvinylidenefluoride (PVDF) copolymer as the matrix.[36] Ghosh *et al.* developed a new transparent conductor comprising AgNWs embedded in an ultrathin polyimide (PI) foil that presents a sheet resistance of 15 ohm sq^{-1} and a very small thickness of 5 μm.[37] The transparent conductive performance is strongly related to the dispersion state of conductive nanomaterials and their conductive network integrity. NFC has been reported to be an efficient dispersant for carbon nanotubes and 2D flakes,[38–40] and then provides the possibility of incorporating with conductive nanomaterials to construct uniformly heterogeneous interlaced network architectures. Transparent hybrid NFC nanopaper with multi-functional properties was prepared by a mimicking solution-based papermaking process, in which the aqueous NFC suspensions were dewatered through evaporation or vacuum filtration, followed by oven drying or hot pressing.[41,42] In our previous work,[43–45] we developed a pressured-extrusion papermaking process for the fast fabrication of luminescent NFC nanopaper with high transparency (over 90%). Highly oriented fibrous networks combined with various functional guest materials were admirably obtained after a quick pressured dewatering process.

Herein, ultrathin, highly flexible, conductive and transparent bamboo/hemp NFC/AgNW hybrid nanopaper of 4.5 μm in thickness was successfully assembled using a solution-based pressured-extrusion paper-making process under 0.6 MPa of N_2 gas. The AgNWs were encapsulated under the surface of a multiscale BNFC/HNFC fibrous network using HPMC as a cross-linker. The ultrathin BNFC/HNFC/AgNW nanopaper exhibited a sheet resistance of 1.90 ohm sq^{-1} with a transmittance of 86.41% at 550 nm. Moreover, the strong adhesion and mechanical robustness of the hybrid nanopaper after peeling, bending and folding tests were also investigated in detail. Owing to their outstanding synergistic properties, biomass based hybrid nanopaper combined with AgNWs will show great potential for application in versatile electronic devices, such as flexible displays, touch screens, solar cells and other devices.

Experimental

Materials

Sackcloth made from hemp fiber was collected from the packaging industry and mechanically crushed to small fragments. Bamboo fiber was purchased from Fujian Jianzhou Bamboo Development Co., Ltd. A silver nanowire suspension (0.3 wt%) with an average diameter of 50 nm and an average length of 20–30 μm was synthesized in our laboratory. Sodium hydroxide (NaOH), acetic acid (HAc) and sodium chlorite ($NaClO_2$) were purchased from Chemical Reagent Co., Ltd. Hydroxypropylmethyl cellulose I (HPMC) with a viscosity of 4000 mPa s^{-1} was purchased from Aladdin Chemistry. All chemicals were of analytical grade and used without any further modification.

Preparation of NFC hydrogels

Hemp fiber and bamboo fiber were used as source materials to prepare NFC suspensions. The preparation procedure was as follows. First, 10.0 g of the raw materials were pretreated and swelled with 3 wt% aqueous NaOH solution (300 g) at 80 °C for 4 h and filtered with deionized water until pH ~ 7 to remove dissociative lignin and some pectin. Then, the cellulosic materials were bleached at 100 °C in 0.7 wt% aqueous $NaClO_2$ solution adjusted to neutral pH by using HAc for 2 h with constant stirring, followed by filtration and washing. After decoloration, the mixtures were centrifuged several times at 5000 rpm to remove excess liquid until reaching neutral pH, and subsequently ultrasonically smashed with a high frequency ultrasonic cell crusher (HighNova Instrument Co., Ltd) at 1000 W for 0.5 h. Finally, hemp NFC (HNFC) and bamboo NFC (BNFC) hydrogels were successfully synthesized after being further refined by a homogenization process with a high pressure homogenizer (D-3L, PhD Technology LLC, USA) for 3 cycles at a pressure of 172 MPa.

Preparation of NFC/AgNW hybrid suspensions

HNFC hydrogels, BNFC hydrogels and HNFC/BNFC hybrid hydrogels were firstly ultrasonically dispersed in 100 g deionized water for 15 min to form 0.5 wt% aqueous suspensions, respectively. Then, AgNW suspension (0.3 wt%) was slowly added to NFC suspensions in a given ratio under magnetic stirring for 1 h. Finally, 0.3 g HPMC dissolved in distilled water (0.35 wt%) was introduced into the aforementioned suspension to obtain uniformly blended dispersions, named BNFC/AgNW suspension, HNFC/AgNW suspension and BNFC/HNFC/AgNW suspension, respectively.

Fabrication of NFC/AgNW hybrid nanopaper

The as-prepared hybrid suspensions were poured into the extruder (NanoAble-150, PhD Technology LLC, USA) to remove excess water under 0.6 MPa of N_2 gas for 40 min using a nuclepore track-etch filter membrane (200 nm PC, Whatman, UK). After extrusion, the wet film was carefully peeled off from the PC filter membrane, sandwiched between two pieces of glass sheets and then dried at 125 °C for 10 min. The NFC/AgNW hybrid nanopapers of 45 mm in diameter were ultimately fabricated (hereinafter referred to as BNFC/AgNW nanopaper, HNFC/AgNW nanopaper and BNFC/HNFC/AgNW nanopaper, respectively). The schematic diagram of the solution-processed procedures of NFC/AgNW nanopaper is shown in Scheme 1.

Instruments and characterization

The morphologies of NFC and AgNWs were measured by transmission electron microscopy (TEM) (JEM-2010F, JEOL, Japan) operated at a 120 kV accelerating voltage. The surface

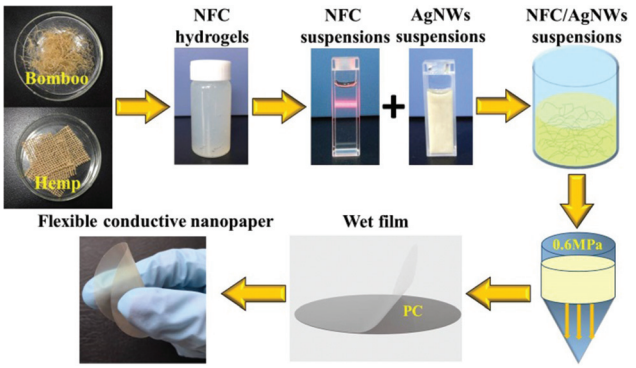

Scheme 1 The schematic diagram of the solution-processed procedures of NFC/AgNW nanopaper.

morphologies of the as-prepared NFC/AgNW nanopaper were observed using a field emission-scanning electron microscope (SEM) (S-4800, Hitachi, Japan) and an atomic force microscope (AFM) (Veeco Dimension 3100). The phase structures of the NFC/AgNW nanopaper were characterized by powder X-ray diffraction (XRD) (D/max 2550, Rigaku, Japan) operating at 40 kV and 40 mA. The sheet resistance (R_s) of the NFC/AgNWs was tested using the standard four probe technique (RTS-8, China) and the measurements were averaged for 3 replicates. The optical transmittance measurement of the hybrid film was carried out on a UV–Vis spectrophotometer (2501PC, Shimadzu, Japan). The thermal stability of the NFC/AgNW nanopaper was studied using a thermogravimetric analyzer (TGA, STA409PC, Netzsch, Germany) at a heating rate of 10 °C min^{-1} in the range of 30–900 °C under a nitrogen atmosphere.

Results and discussion

The appearance of isolated NFC suspensions has a bright channel when shining light with a laser beam (Scheme 1), called the "Tyndall effect". It can be concluded that the colloidal suspensions are very stable and the sizes of NFC are all on the nanometric scale. The morphologies clearly discerned from the TEM images shown in Fig. 1 indicate that the BNFC has a narrower size distribution than that of HNFC. The BNFC is mainly composed of nanofibers of 10–15 nm in diameter and 500–1000 nm in length (Fig. 1a), while HNFC ranges from 20 nm to 50 nm in diameter and 1000–2000 nm in length (Fig. 1b). The results indicated that regular bamboo fiber and hemp fiber were successfully disintegrated into nanocrystalline cellulose with an average diameter of tens of nanometers and a length of hundreds of nanometers to several micrometers after chemical cleavage of amorphous non-cellulosic regions. As the fiber diameter is smaller than 50 nm, NFC will act as an excellent building block for developing a transparent platform with tailored optical and mechanical properties.[46] Fig. 1c displays a TEM image of the BNFC/HNFC/AgNW composites. Blended BNFC/HNFC is blurry in the image because of its smaller size and deficient crystallinity compared to AgNWs. The image shows that different sizes of BNFC/HNFC conjoin together to form a fibrous network structure. It is obvious that the well-dispersed AgNWs are closely combined with the BNFC/HNFC fibrous network. The tangled fibrous network is beneficial for expanding the pathway of AgNWs to make them fully contact for establishing an electrical network.

Digital pictures of BNFC/HNFC/AgNW hybrid nanopaper obtained by using the pressured-extrusion process are presented in Fig. 2. It is obvious that the hybrid nanopaper displays high optical transparency, indicating that the uniform combination of AgNWs with BNFC/HNFC reduces light scattering of the hybrid nanopaper. However, the transmittance of the hybrid nanopaper decreases with the increase of the stoi-

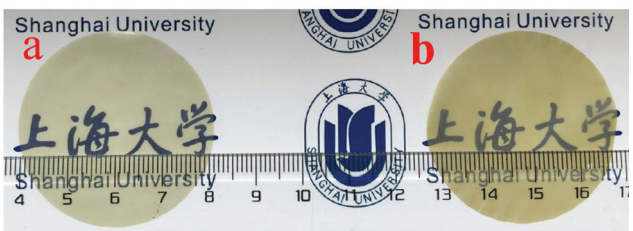

Fig. 2 Digital pictures of BNFC/HNFC/AgNW hybrid nanopaper with a weight ratio of BNFC/HNFC to AgNWs of (a) 1 : 0.4 and (b) 1 : 1.

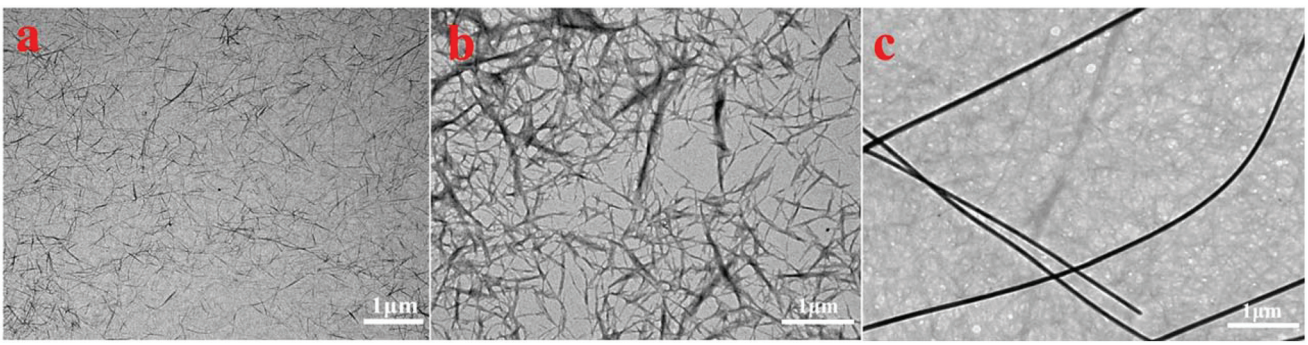

Fig. 1 TEM images of (a) BNFC, (b) HNFC and (c) BNFC/HNFC/AgNW.

This journal is © The Royal Society of Chemistry 2015

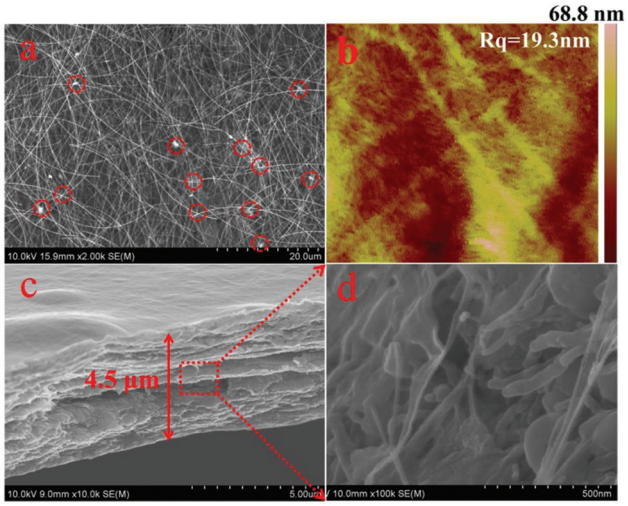

Fig. 3 (a) Top-view FE-SEM image and (b) AFM image of the BNFC/HNFC/AgNW hybrid nanopaper with a weight ratio of BNFC/HNFC to AgNWs of 1 : 1. (c and d) Cross-sectional SEM images of BNFC/HNFC/AgNW hybrid nanopaper.

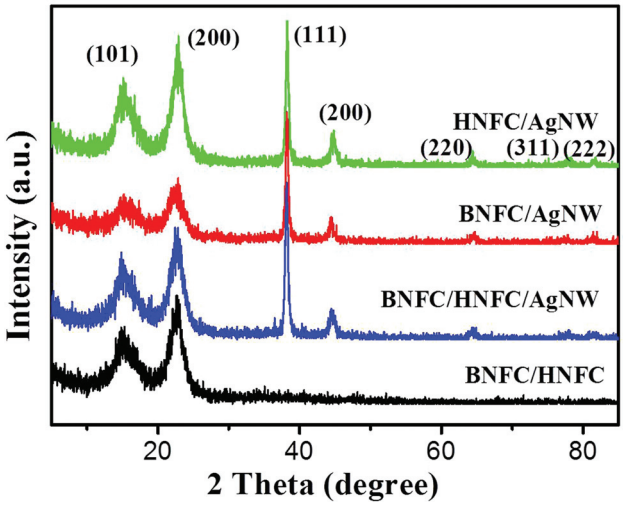

Fig. 4 XRD patterns of BNFC/HNFC, BNFC/AgNW, HNFC/AgNW, and BNFC/HNFC/AgNW hybrid nanopapers.

chiometric ratio of BNFC/HNFC to AgNWs from 1 : 0.4 to 1 : 1. This result is verified from the school emblem of Shanghai University under the hybrid films which becomes more obscure. SEM and AFM images of the surface and fracture section of BNFC/HNFC/AgNW hybrid nanopaper are presented in Fig. 3. It can be obviously observed, from the top-view FE-SEM image shown in Fig. 3a, that the AgNWs appear to be more uniformly distributed in the BNFC/HNFC substrate by intertwining with each other.[32,47] Therefore, a closely packed electrical network structure was constructed after a pressured-extrusion to remove excess water. The fast dewatering process is an efficient paper-making method for using well dispersed hybrid suspensions to quickly fabricate a physically compact nanopaper with uniformly heterogeneous fibrous network architecture because of drainage in the perpendicular direction through the plenty of nanopores in the paper matrix.[32] It can be clearly demonstrated that the AgNW junctions are soldered by BNFC/HNFC using HPMC as the cross-linker (red circles in Fig. 3a). The knotted AgNW junctions are beneficial to reduce inter-nanowire contact resistance and greatly enhance the electrical conductivity.[48,49] The long AgNWs render a significant electrical network while still enabling high optical transparency for hybrid nanopaper. It can also be seen from an AFM height image (Fig. 3b) that AgNWs are well dispersed in a NFC matrix. The fact that the AgNWs were embedded under the surface of hybrid nanopaper without large surface roughness was clearly confirmed by a 3D AFM image (see ESI, Fig. S1†). The fibrous nature of the nanopaper is further verified by the cross-sectional SEM images shown in Fig. 3c and d; it can be observed that the well-stacked nanopaper of 4.5 μm in thickness represents a poriferous fibrous structure combined with NFC and AgNW blended fibers perpendicular to the breaking direction. It can be deduced that the nanofibrous bundles may be strongly linked together to display excellent mechanical properties of the BNFC/HNFC/AgNW hybrid nanopaper.

The phase structure and composition of hybrid nanopaper were further analysed by XRD measurements. As revealed in Fig. 4, the peaks at 16.4° and 22.4° can be indexed to the typical (101) and (200) reflections of cellulose I. Except for characteristic peaks of NFC, all the other diffraction peaks at 38.12°, 44.32°, 65.54°, 77.40°, 81.53° are attributed to the diffraction of the (111), (200), (220), (311) and (222) crystal planes of the face-centered cubic silver (no. 04-0783), respectively. It is convincingly implied that the as-prepared hybrid nanopaper is composed of cellulose and silver composites.

Fig. 5 shows the transparent conductive performances of HNFC/AgNW and BNFC/HNFC/AgNW hybrid nanopaper under the same conditions. A commercial ITO/PET conductive film was also evaluated as a reference. The ITO/PET film shows a sheet resistance of 11.50 ohm sq^{-1} and a $T_{550\ nm}$ of 94.01%. It is obviously observed that BNFC/HNFC/AgNW hybrid nanopaper displays much higher performance than HNFC/AgNW hybrid nanopaper with the same additive amount of AgNWs. The sheet resistance of BNFC/HNFC/AgNW hybrid nanopaper (Fig. 1b) is 1.90 ohm sq^{-1} at a wavelength of 550 nm, which is nearly 95 times lower than that of HNFC/AgNW hybrid nanopaper. The difference perhaps comes from the different homogeneity of the electrical network. In a regular paper structure, all the fibers are arranged into a random fibrous network with lots of air cavities.[50] Therefore careful attention must be paid to how homogeneity is manipulated using different sizes of fibers to establish a uniformly heterogeneous multi-scale framework. So the ambition is to integrate AgNWs (50 nm in diameter), HNFC (20–50 nm in diameter) and BNFC (10–15 nm in diameter) together to construct a strong interlaced BNFC/HNFC/AgNW ternary system, where it is assumed that the cavities between larger HNFC and AgNWs were

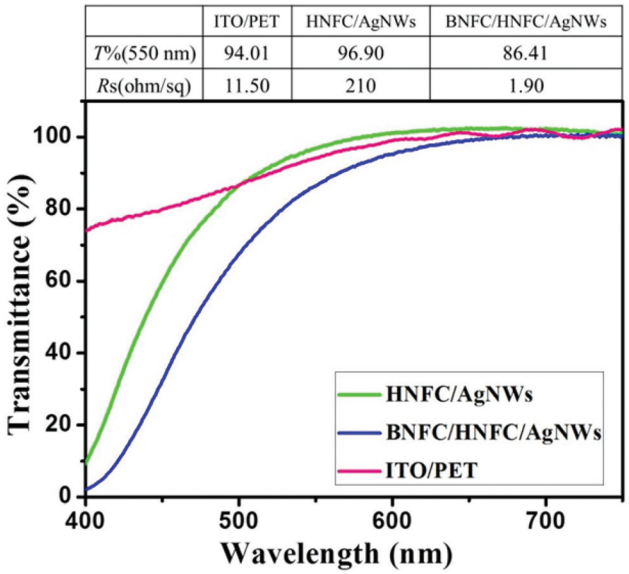

Fig. 5 Transparent conductive performance of HNFC/AgNW and BNFC/HNFC/AgNW transparent papers and ITO/PET film.

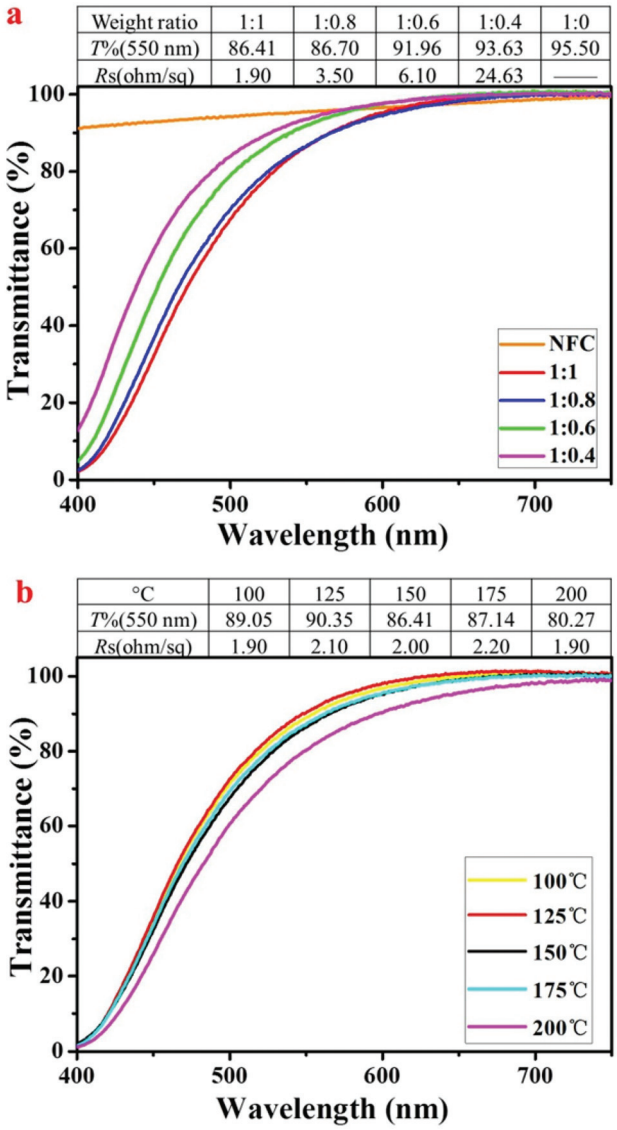

Fig. 6 (a) Transparent conductive performance of BNFC/HNFC/AgNW transparent paper with different AgNW dosages; (b) transparent conductive performance of BNFC/HNFC/AgNW transparent paper with a weight ratio of BNFC/HNFC to AgNWs of 1 : 1 under different drying temperatures.

thoroughly filled by smaller BNFC and the connection was subsequently reinforced to form an interpenetrating electrical network.

BNFC/HNFC/AgNW hybrid nanopaper comprising various weight ratios of AgNWs (BNFC/HNFC to AgNWs; 1 : 1, 1 : 0.8, 1 : 0.6, and 1 : 0.4) are demonstrated in Fig. 6. Each hybrid nanopaper has equal amounts of BNFC and HNFC. The gradual addition of larger sized AgNWs increases light scattering and then decreases optical transparency. The transmittance of pure BNFC/HNFC nanopaper without AgNWs is 95% at a wavelength of 550 nm. It is evident that optical transmittance increases with the decrease of the AgNW concentration, as shown in Fig. 6a. For the BNFC/HNFC/AgNW hybrid nanopaper with a weight ratio of 1 : 0.4, the optical transmittance reaches 93.63% (at 550 nm) with a sheet resistance of 24.63 ohm sq^{-1}. When the weight ratio of BNFC/HNFC to AgNWs is 1 : 1, the optical transmittance of the hybrid nanopaper decreases to 86.41% and the sheet resistance dramatically reduces to 1.90 ohm sq^{-1}, equal to the electronic conductivity, which is about 500 S cm^{-1}.

The effect of drying temperature on the transparent conductive performances of BNFC/HNFC/AgNW hybrid nanopaper was also investigated. Fig. 6b shows the optical transmittance and sheet resistance of BNFC/HNFC/AgNW hybrid nanopaper at different drying temperatures ranging from 100 to 200 °C. The hybrid nanopaper displays the best performances with the optical transmittance of 90.35% at a drying temperature of 125 °C. With the drying temperature rising constantly, the surface smoothness will be reduced due to the excessive thermal evaporation. The rough surface after higher drying temperature may contribute to an enhancement of light scattering and a decrease of specular transmittance. Interestingly, the sheet resistances of all the hybrid nanopapers were little changed. Therefore, their outstanding performances are much better than those of ITO plastic films, indicating that the hybrid nanopaper with an appropriate amount of AgNWs providing an efficiently connected electrical network will meet the optoelectronic requirements for touch screen panels or solar cells. The initial degradation temperature was 300 °C, which was much higher than the conventional application temperature of conductive plastic films (see ESI, Fig. S2†). If a PET film is held at 150 °C for tens of minutes, the surface roughness will increase, thus resulting in the decrease of optical transparency.[51]

This journal is © The Royal Society of Chemistry 2015

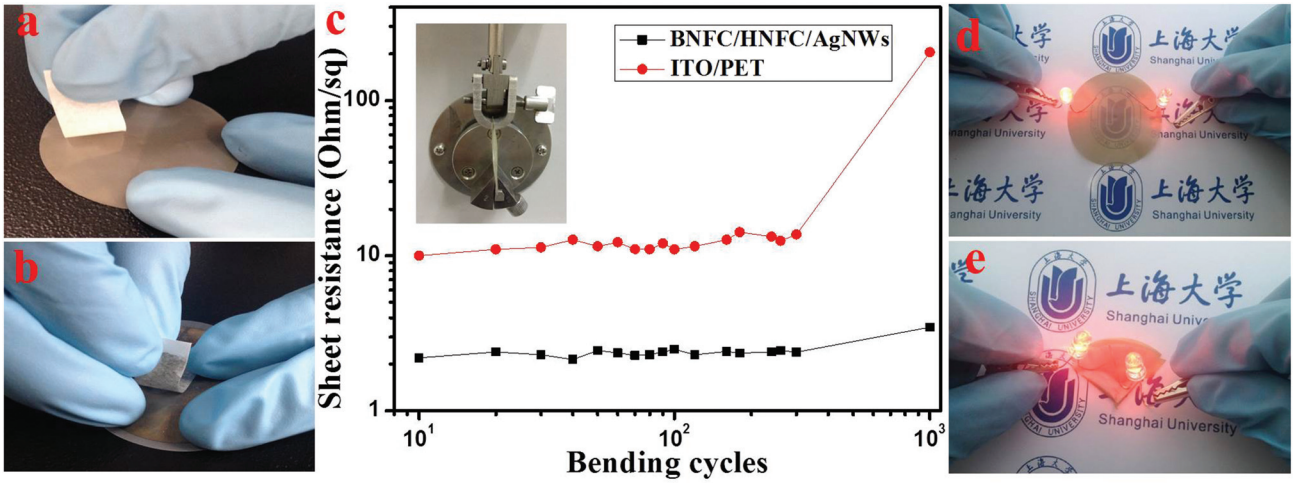

Fig. 7 Digital pictures of (a) BNFC/HNFC/AgNW hybrid nanopaper and (b) AgNWs deposited on the PET substrate after the peeling test; (c) sheet resistance of BNFC/HNFC/AgNW hybrid nanopaper and the commercial ITO/PET film as a function of bending cycles, the inset shows an image of the bending test machine used; and the lighting of two light-emitting diodes (LED, 3 V) placed between the BNFC/HNFC/AgNW hybrid nanopaper (d) before and (e) after bending at 135° for 1000 cycles.

Owing to the structural advantages and extraordinary electrical conductivity of the ternary network system, BNFC/HNFC/AgNW hybrid nanopaper exhibited excellent mechanical robustness against adhesion, friction and bending, and can be used as a prospective candidate for flexible and stretchable conductors. Fig. 7a shows the digital pictures of the hybrid nanopaper with a weight ratio of BNFC/HNFC to AgNWs of 1 : 1 using adhesive tape for the peeling test. The performance of hybrid nanopaper with superior adhesion was maintained even after the peeling off test for 60 cycles (see ESI, Fig. S3†). In contrast, AgNWs deposited on the PET film (Fig. 7b) were easily peeled off from the substrate.[7,8] It can be noted that the AgNW fragile network intrinsically anchored into the BNFC/HNFC matrix becomes mechanically flexible, as shown in Fig. 7c. The electrical resistance was negligibly changed after bending at 135° for 1000 cycles, whereas the sheet resistance of the commercial ITO/PET conductive film was drastically increased by more than 10 times after the same bending cycles. In addition, the BNFC/HNFC/AgNW hybrid nanopaper was successfully used to light a light-emitting diode (LED, 3 V). It is obvious that the LEDs still give off bright light even after bending for 1000 cycles (Fig. 7d and e). Moreover, the hybrid nanopaper exhibited an excellent morphological stability after folding, whereas the commercial ITO/PET conductive film displayed lots of microscopic cracks along the direction perpendicular to that of folding stress due to the stiff ITO coating (see ESI, Fig. S4†). The results further confirm that the conductive hybrid nanopaper has excellent mechanical durability performance. Hence, it can be concluded that the AgNW junctions were embedded into BNFC/HNFC to form a stable multiscale heterogeneous electrical network with strong adhesion and outstanding mechanical flexibility.

Conclusions

In summary, we have successfully fabricated an ultrathin, highly transparent conductive nanopaper using a solution-based pressured-extrusion aqueous paper-making process under 0.6 MPa of N_2 gas. The hybrid nanopaper was quickly assembled with bamboo/hemp NFC as a fibrous network, AgNWs as conductive fillers and HPMC as a cross-linker. Thus AgNWs were encapsulated into the BNFC/HNFC fibrous network and then a uniform multiscale heterogeneous electrical network architecture was ultimately established. The ultrathin BNFC/HNFC/AgNW hybrid nanopaper of 4.5 μm in thickness demonstrated excellent transparent conductive performance and strong mechanical durability. The hybrid nanopaper possesses high optical transmittance (86.41% at 550 nm), low sheet resistance (1.90 ohm sq^{-1}), and strong adhesion and mechanical flexibility, and can be used to fabricate efficient, flexible and printable paper electronic devices for future applications. On the basis of the solution-processed method and easy recyclability, cellulose based transparent nanopaper shows promising potential for application in eco-friendly, portable and easily up-scalable device production that outperforms ITO/PET based devices.

Acknowledgements

This work was financially supported by the Science and Technology Commission of Shanghai Municipality (13ZR1415100, 15ZR1415100, and 13JC1402700). The authors are also grateful to Instrumental Analysis & Research Center of Shanghai University.

Notes and references

1 M. Österberg, J. Vartiainen, J. Lucenius, U. Hippi, J. Seppälä, R. Serimaa and J. Laine, *ACS Appl. Mater. Interfaces*, 2013, **5**, 4640–4647.
2 B. D. Gates, *Science*, 2009, **323**, 1566–1567.
3 M. Henriksson, L. A. Berglund, P. Isaksson, T. Lindström and T. Nishino, *Biomacromolecules*, 2008, **9**, 1579–1585.
4 J. Kang, Y. Jang, Y. Kim, S.-H. Cho, J. Suhr, B. H. Hong, J.-B. Choi and D. Byun, *Nanoscale*, 2015, **7**, 6567–6573.
5 H. Sehaqui, Q. Zhou, O. Ikkala and L. A. Berglund, *Biomacromolecules*, 2011, **12**, 3638–3644.
6 H. L. Zhu, B. B. Narakathu, Z. Q. Fang, A. T. Aijazi, M. Joyce, M. Atashbar and L. B. Hu, *Nanoscale*, 2014, **6**, 9110–9115.
7 D. Lee, H. Lee, Y. Ahn and Y. Lee, *Carbon*, 2015, **81**, 439–446.
8 D. Paeng, J.-H. Yoo, J. Yeo, D. Lee, E. Kim, S. H. Ko and C. P. Grigoropoulos, *Adv. Mater.*, 2015, **27**, 2762–2767.
9 D. S. Hecht, L. Hu and G. Irvin, *Adv. Mater.*, 2011, **23**, 1482–1513.
10 H. Kang, S. Jung, S. Jeong, G. Kim and K. Lee, *Nat. Commun.*, 2015, **6**, 6503.
11 D. J. Lipomi, J. A. Lee, M. Vosgueritchian, B. C. K. Tee, J. A. Bolander and Z. Bao, *Chem. Mater.*, 2012, **24**, 373–382.
12 M. Vosgueritchian, D. J. Lipomi and Z. Bao, *Adv. Funct. Mater.*, 2012, **22**, 421–428.
13 K. S. Kim, Y. Zhao, H. Jang, S. Y. Lee, J. M. Kim, K. S. Kim, J.-H. Ahn, P. Kim, J.-Y. Choi and B. H. Hong, *Nature*, 2009, **457**, 706–710.
14 D. Lee, H. Lee, Y. Ahn and Y. Lee, *Carbon*, 2015, **81**, 439–446.
15 K.-Y. Shin and J. Jang, *Chem. Commun.*, 2014, **50**, 6645–6648.
16 Y. C. Jung, D. Shimamoto, H. Muramatsu, Y. A. Kim, T. Hayashi, M. Terrones and M. Endo, *Adv. Mater.*, 2008, **20**, 4509–4512.
17 H. W. Gu and T. M. Swager, *Adv. Mater.*, 2008, **20**, 4433–4437.
18 Z. C. Wu, Z. H. Chen, X. Du, J. M. Logan, J. Sippel, M. Nikolou, K. Kamaras, J. R. Reynolds, D. B. Tanner, A. F. Hebard and A. G. Rinzler, *Science*, 2004, **305**, 1273–1276.
19 S. SeobáLee and S. HwanáKo, *Nanoscale*, 2012, **4**, 6408–6414.
20 J. Lee, S. Connor, Y. Cui and P. Peumans, *Nano Lett.*, 2008, **8**, 689–692.
21 S. De, T. M. Higgins, P. E. Lyons, E. M. Doherty, P. N. Nirmalraj, W. J. Blau, J. J. Boland and J. N. Coleman, *ACS Nano*, 2009, **3**, 1767–1774.
22 L. B. Hu, H. S. Kim, J.-Y. Lee, P. Peumans and Y. Cui, *ACS Nano*, 2010, **4**, 2955–2963.
23 M. Song, D. S. You, K. Lim, S. Park, S. Jung, C. S. Kim, D. H. Kim, D. G. Kim, J. K. Kim and J. Park, *Adv. Funct. Mater.*, 2013, **23**, 4177–4184.
24 C.-H. Liu and X. Yu, *Nanoscale Res. Lett.*, 2011, **6**, 75.
25 S. J. Lee, Y.-H. Kim, J. K. Kim, H. Baik, J. H. Park, J. Lee, J. Nam, J. H. Park, T.-W. Lee, G.-R. Yi and J. H. Cho, *Nanoscale*, 2014, **6**, 11828–11834.
26 T. Tokuno, M. Nogi, M. Karakawa, J. Jiu, T. T. Nge, Y. Aso and K. Suganuma, *Nano Res.*, 2011, **4**, 1215–1222.
27 Y. Liu, X. L. Zhao, B. Cai, T. F. Pei, Y. H. Tong, Q. X. Tang and Y. C. Liu, *Nanoscale*, 2014, **6**, 1323–1328.
28 D. Y. Choi, H. W. Kang, H. J. Sung and S. S. Kim, *Nanoscale*, 2013, **5**, 977–983.
29 P. Lee, J. Ham, J. Lee, S. Hong, S. Han, Y. D. Suh, S. E. Lee, J. Yeo, S. S. Lee, D. Lee and S. H. Ko, *Adv. Funct. Mater.*, 2014, **24**, 5671–5678.
30 L. B. Hu, H. Wu, F. L. Mantia, Y. Yang and Y. Cui, *ACS Nano*, 2010, **4**, 5843–5848.
31 H. Koga, M. Nogi, N. Komoda, T. Nge, T. Sugahara and K. Suganuma, *NPG Asia Mater.*, 2014, **6**, e93.
32 J. Jiu, M. Nogi, T. Sugahara, T. Tokuno, T. Araki, N. Komoda, K. Suganuma, H. Uchida and K. Shinozaki, *J. Mater. Chem.*, 2012, **22**, 23561–23567.
33 J. Li, W. N. Zhang, Q. G. Li and B. J. Li, *Nanoscale*, 2015, **7**, 2889–2893.
34 Q. S. Xu, W. F. Shen, Q. J. Huang, Y. Yang, R. Q. Tan, K. Zhu, N. Dai and W. J. Song, *J. Mater. Chem. C*, 2014, **2**, 3750–3755.
35 C. Preston, Z. Q. Fang, J. Murray, H. L. Zhu, J. Q. Dai, J. N. Munday and L. B. Hu, *J. Mater. Chem. C*, 2014, **2**, 1248–1254.
36 K.-Y. Chun, Y. Oh, J. Rho, J.-H. Ahn, Y.-J. Kim, H. R. Choi and S. Baik, *Nat. Commun.*, 2010, **5**, 853–857.
37 D. S. Ghosh, T. L. Chen, V. Mkhitaryan and V. Pruneri, *ACS Appl. Mater. Interfaces*, 2014, **6**, 20943–20948.
38 Z. Q. Fang, H. L. Zhu, Y. B. Yuan, D. Ha, S. Zhu, C. Preston, Q. X. Chen, Y. Y. Li, X. G. Han, S. Lee, G. Chen, T. Li, J. Munday, J. S. Huang and L. B. Hu, *Nano Lett.*, 2014, **14**, 765–773.
39 N. T. Cervin, L. Andersson, J. B. S. Ng, P. Olin, L. Bergström and L. Wågberg, *Biomacromolecules*, 2013, **14**, 503–511.
40 Y. Y. Li, H. L. Zhu, F. Shen, J. Y. Wan, S. Lacey, Z. Q. Fang, H. Q. Dai and L. B. Hu, *Nano Energy*, 2015, **13**, 346–354.
41 Z. Weng, Y. Su, D.-W. Wang, F. Li, J. Du and H.-M. Cheng, *Adv. Energy Mater.*, 2011, **1**, 917–922.
42 H. Sehaqui, A. Liu, Q. Zhou and L. A. Berglund, *Biomacromolecules*, 2010, **11**, 2195–2198.
43 M. Miao, J. P. Zhao, X. Feng, Y. Cao, S. M. Cao, Y. F. Zhao, X. Q. Ge, L. N. Sun, L. Y. Shi and J. H. Fang, *J. Mater. Chem. C*, 2015, **3**, 2511–2517.
44 J. P. Zhao, Z. W. Wei, X. Feng, M. Miao, L. N. Sun, S. M. Cao, L. Y. Shi and J. H. Fang, *ACS Appl. Mater. Interfaces*, 2014, **6**, 14945–14951.
45 S. M. Cao, Y. Y. Song, X. Feng, H. J. Liu, M. Miao, J. H. Fang and L. Y. Shi, *ACS Appl. Mater. Interfaces*, 2015, **7**, 10695–10701.
46 H. L. Zhu, S. Parvinian, C. Preston, O. Vaaland, Z. C. Ruan and L. B. Hu, *Nanoscale*, 2013, **5**, 3787–3792.
47 X. Y. Zeng, Q. K. Zhang, R. M. Yu and C. Z. Lu, *Adv. Mater.*, 2010, **22**, 4484–4488.

This journal is © The Royal Society of Chemistry 2015

48 J. Liang, L. Li, K. Tong, Z. Ren, W. Hu, X. Niu, Y. Chen and Q. Pei, *ACS Nano*, 2014, **8**, 1590–1600.
49 J. Lee, P. Lee, H. B. Lee, S. Hong, I. Lee, J. Yeo, S. S. Lee, T.-S. Kim, D. Lee and S. H. Ko, *Adv. Funct. Mater.*, 2013, **23**, 4171–4176.
50 Z. Q. Fang, H. L. Zhu, C. Preston, X. G. Han, Y. Y. Li, S. Lee, X. S. Chai, G. Chen and L. B. Hu, *J. Mater. Chem. C*, 2013, **1**, 6191–6197.
51 M. Nogi, C. Kim, T. Sugahara, T. Inui, T. Takahashi and K. Suganuma, *Appl. Phys. Lett.*, 2013, **102**, 181911.

This journal is © The Royal Society of Chemistry 2015